Split-Phase Control

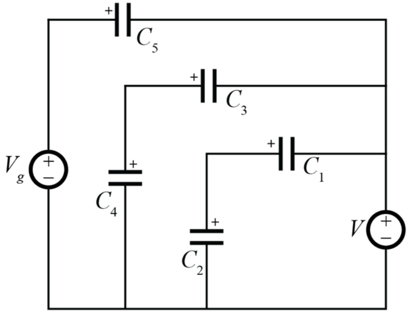

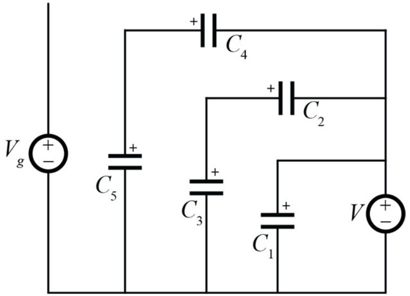

Y. Lei, R. May, and R. Pilawa-Podgurski, "Split-Phase Control: Achieving Complete Soft-Charging Operation of a Dickson Switched- Capacitor Converter," 2016

LTSpice Simulation

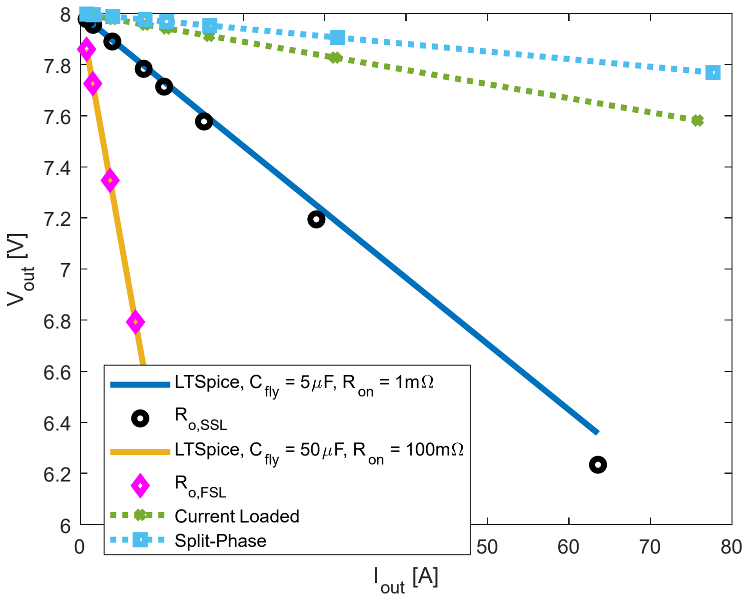

Complete Soft Charging

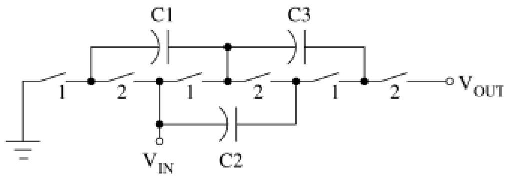

a) Ladder

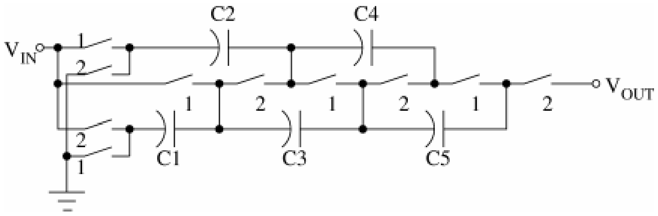

b) Dickson Charge Pump

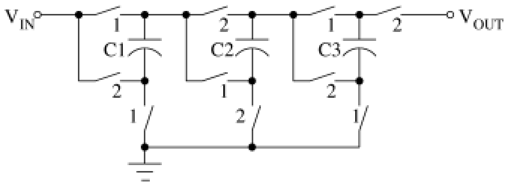

c) Fibonacci

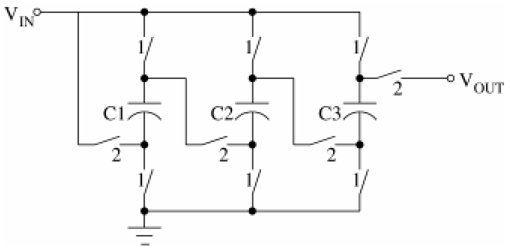

d) Series-Parallel

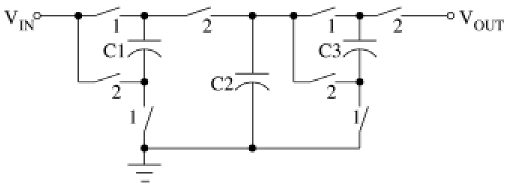

e) Doubler

Y. Lei and R. Pilawa, “A General Method for Analyzing Resonant and Soft-Charging Operation of Switched-Capacitor Converters” TPEL 2014
S. R. Pasternak, M. H. Kiani, J. S. Rentmeister and J. T. Stauth, “Modeling and Performance Limits of Switched-Capacitor DC–DC Converters Capable of Resonant Operation With a Single Inductor”, JESTPE 2017

FCML and SC Buck

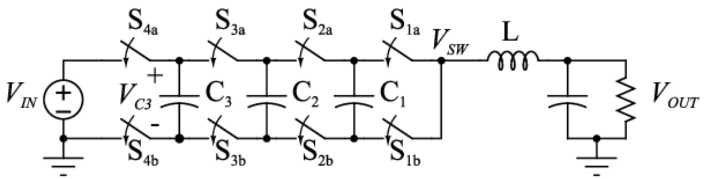

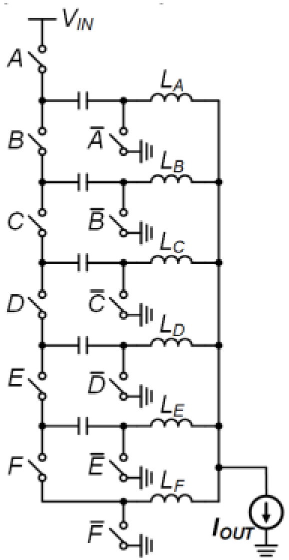

Types of Capacitors

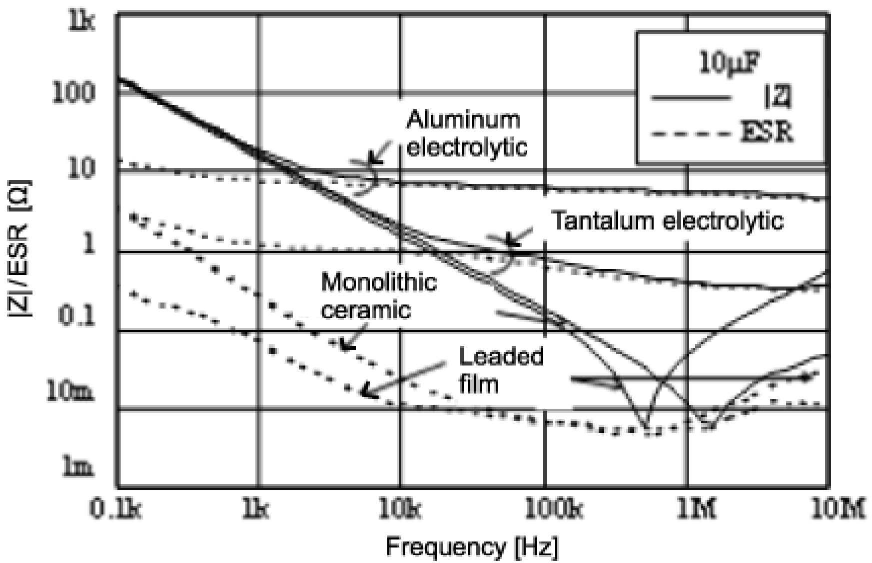

Ceramic Capacitor Impedance and Resistance

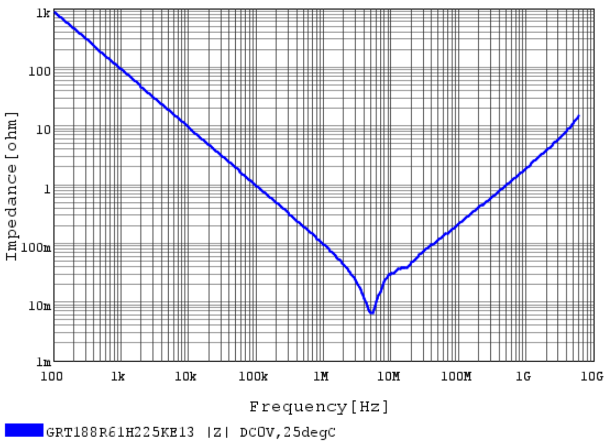

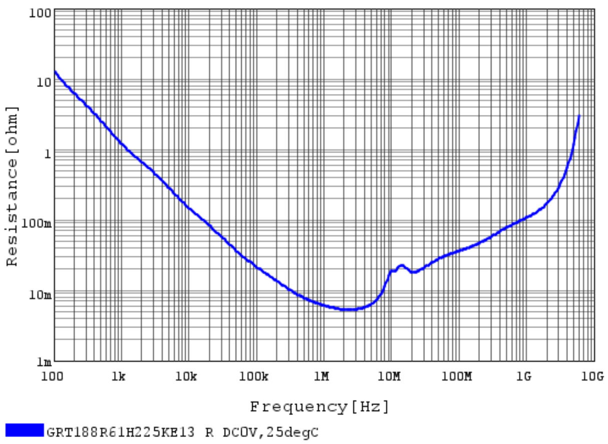

Capacitor data sources

- Murata Simsurfing
- TDK SEAT

MLCC

- Capacitor codes, e.g. X7R or C0G standardized to define stability over temperature
  - **Class-II**: Codes begin with X, Y, or Z (e.g. X7R, Y5V)
  - **Class-I**: Codes begin with [CBLAMPRSTVU] (e.g. C0G, NPO)

2.2µF, 50V X7R (Class-II) 0603 footprint

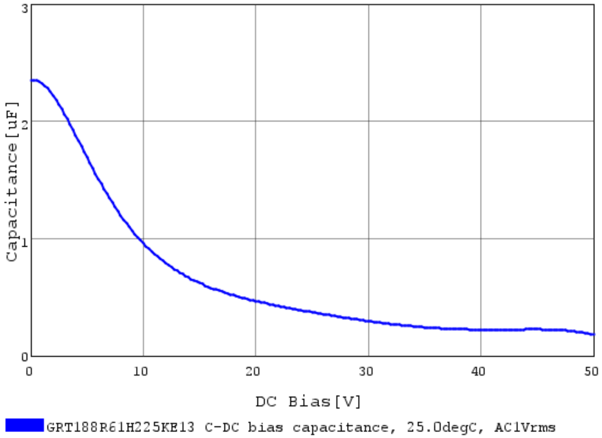

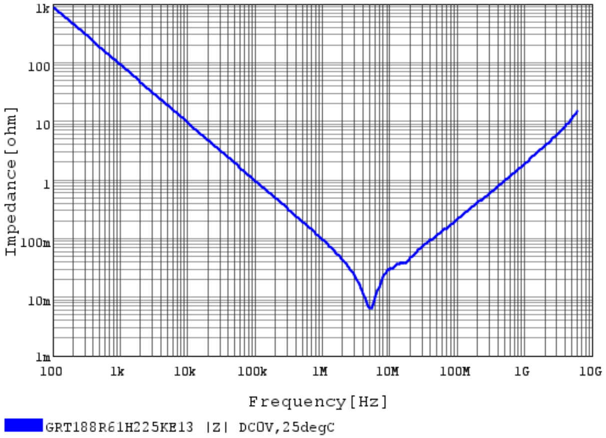

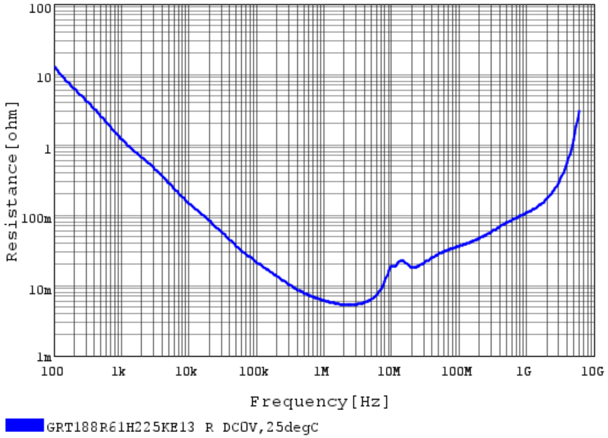

Remaining: 7.2% at full voltage

10nF, 50V C0G (Class-I) 0603 footprint

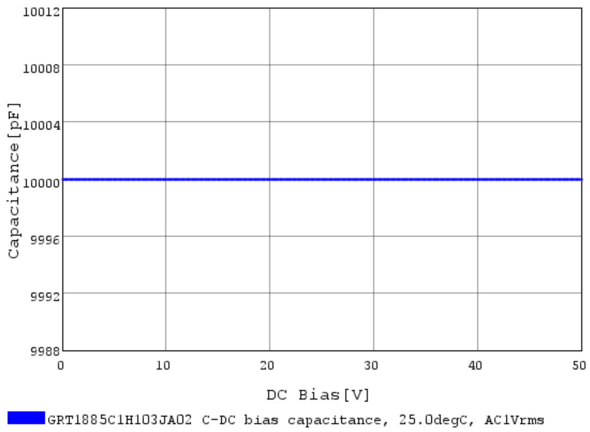

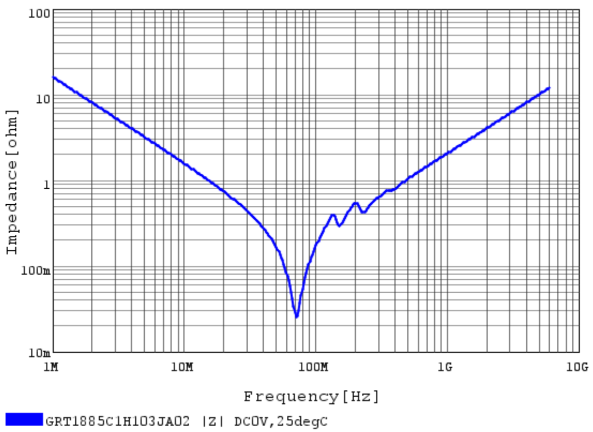

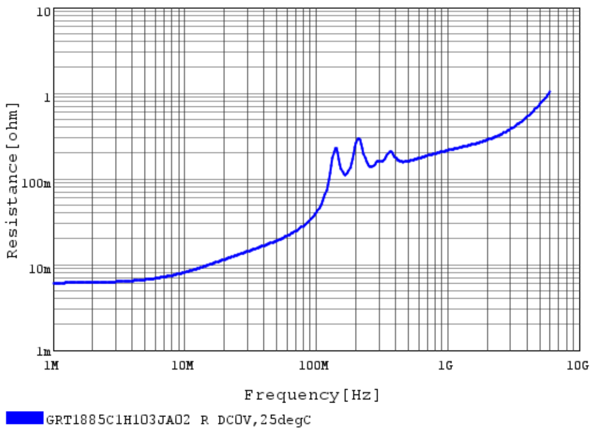

10nF, 50V X7R (Class-II) 0603 footprint

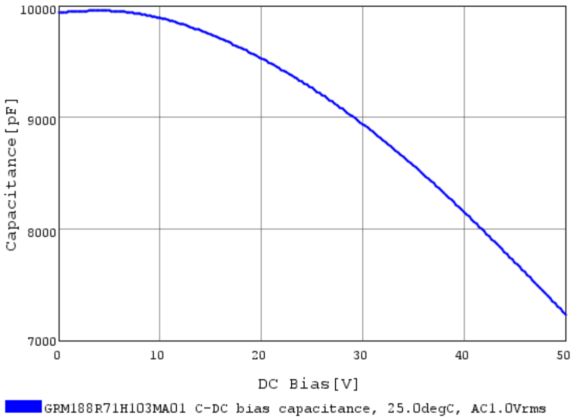

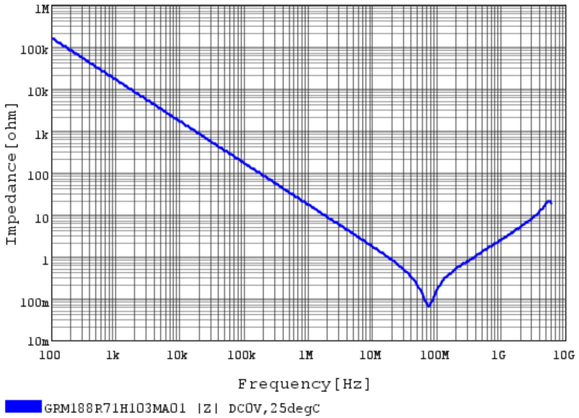

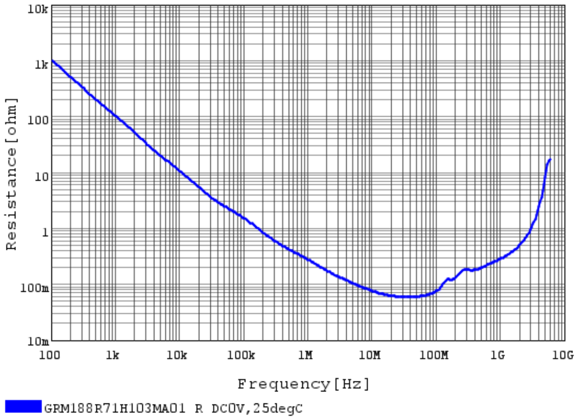

10nF, 50V C0G (Class-I) varied footprint

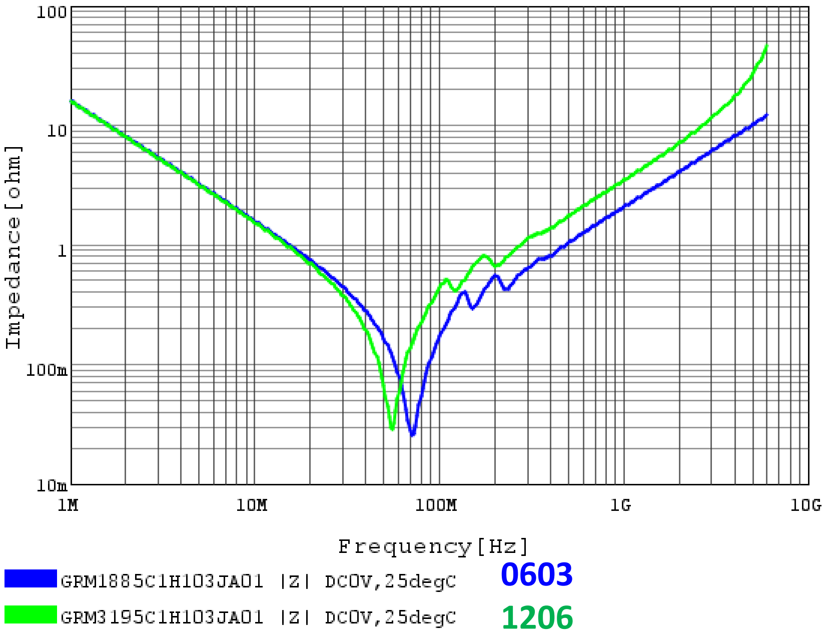

Same 0603 Footprint

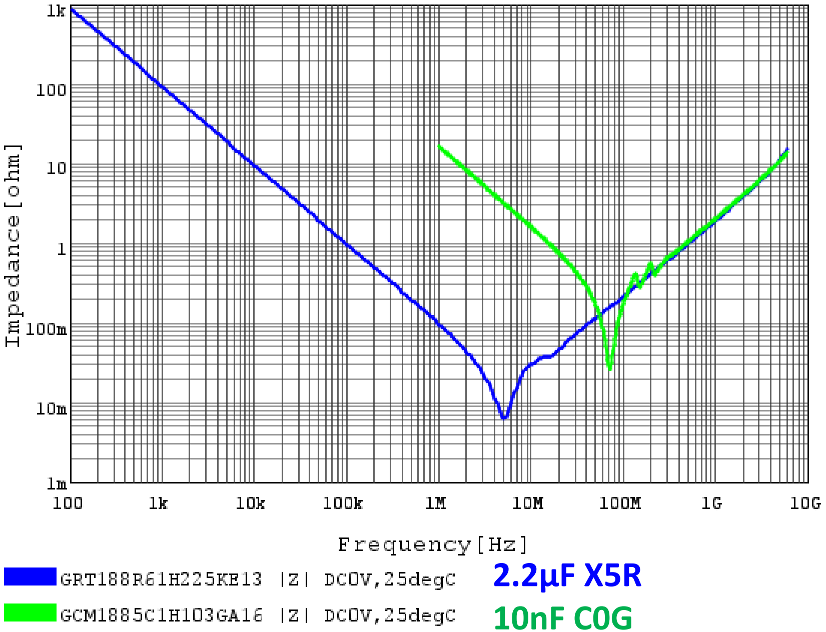

2.2µF X5R

10nF C0G

Class-II Capacitor Hysteresis Loss

TABLE II
EMPLOYED COMPONENTS

Component	Dielectric	Manufacturer	Part Number	V_n	C_n	N(parallel)	C_{tot}	DF
C_{cal}	C0G	TDK	CAA572C0G2J204J640LH	650 V	200 nF	2	400 nF	$< 0.02\,\%$
C_{ref}	C0G	TDK	C5750C0G2A154J230KE	100 V	150 nF	32	4.8 µF	$< 0.03\,\%$
C_{DUT}	X7R	Knowles Syfer	2220Y1K00474KETWS2	1 kV	470 nF	1	470 nF	$> 0.71\,\%$

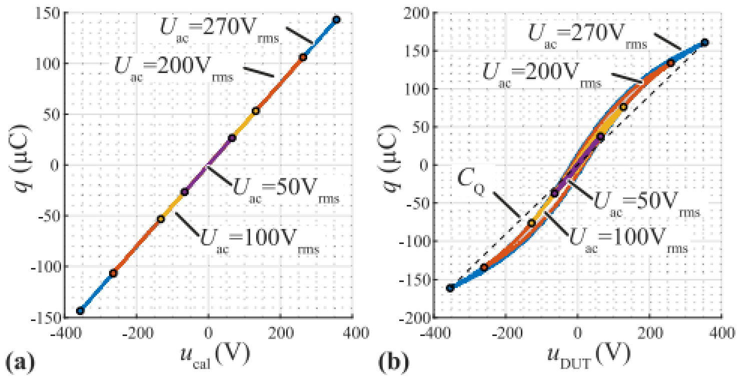

Fig. 6. $U - Q$ hysteresis recorded at 50 Hz for a range of excitation voltages for (a) the calibration capacitor, which shows no hysteresis and has a constant $C_Q = C_d$ at all voltages, and (b) the DUT, which exhibits increasing hysteresis and losses with increasing excitation voltage. C_Q highlighted for U_{ac} =270 V_{rms}. Measured $U - Q$ curves are identical at 50 Hz and 100 Hz.

C_{oss} Hysteresis

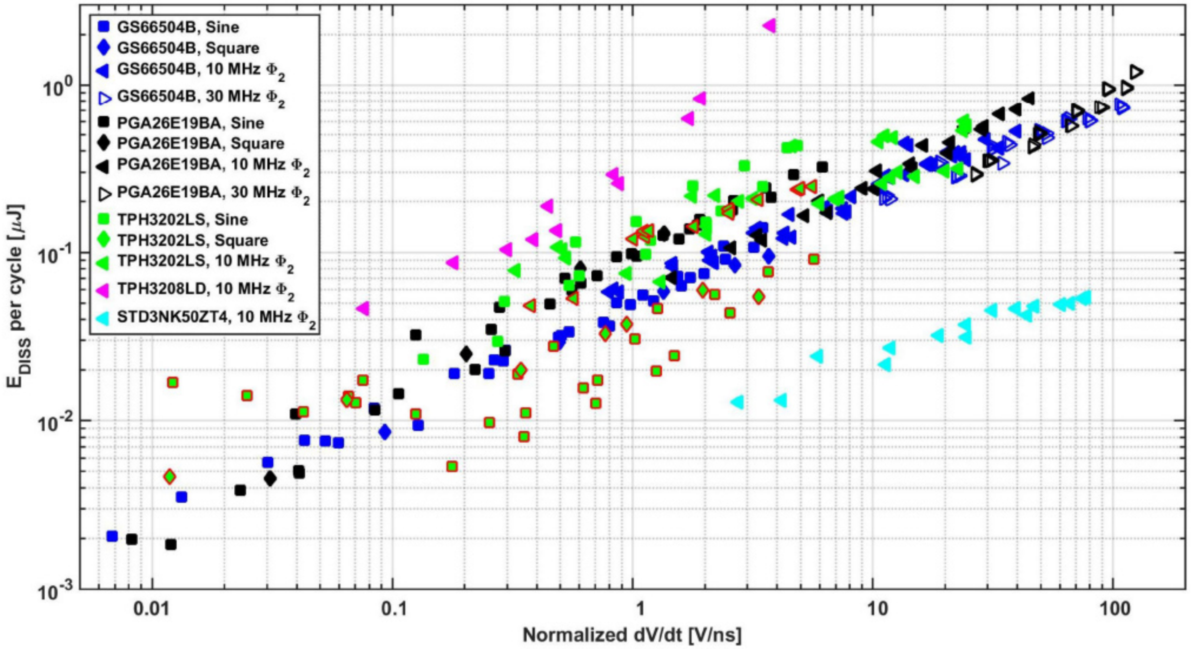

Fig. 15. Losses per cycle versus normalized, by (8), $\mathbf{dV/dt}$ for the three studied devices and two additional "extreme performance" devices. The red outline around the TPH3202LS results indicates applied voltages under 300 V and $\beta = 1.46$ in (8). All recorded measurements are included here. There are no measurements for the TPH3202LS 30 MHz Φ_2, as the Φ_2 wave generator could not be tuned to maintain ZVS with the TPH3202LS device and C_{REF} in parallel.

Transistor Structure and Material

SiC

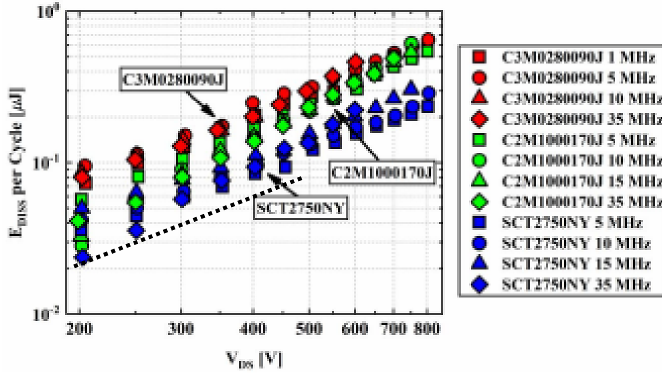

Fig. 4: C_{OSS} losses for three devices from 1-35 MHz.

Si Superjunction

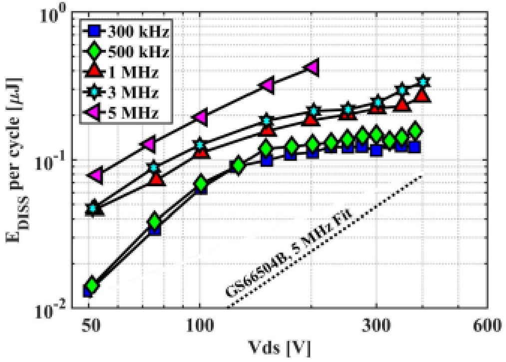

(b) High-frequency C_{OSS} losses for the R6011KNTJL device.

Fig. 6: Silicon superjunction C_{OSS} loss data.

Si

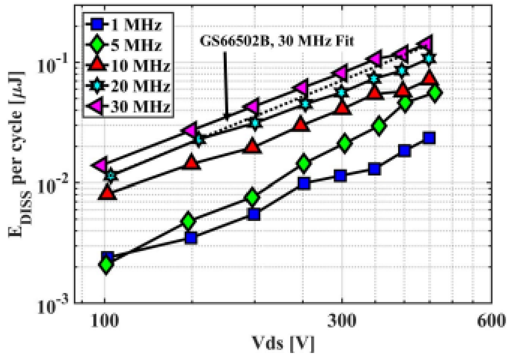

Fig. 7: C_{OSS} losses for STD3NK50ZT4.

G. Zulauf, Z. Tong and J. Rivas-Davila, "Considerations for Active Power Device Selection in High- and Very-High-Frequency Power Converters," COMPEL *2018*